

# Effect of Bonding Temperature on Microstructure Evolution during TLP Bonding of a Ni<sub>3</sub>Al based Superalloy IC10

Xiong Yue<sup>1,2</sup>, Fengmei Liu<sup>1</sup>, Hexing Chen<sup>1</sup>, Di Wan<sup>1</sup> and Hongbo Qin<sup>1</sup>

<sup>1</sup>Guangdong Provincial Key Laboratory of Advanced Welding Technology, Guangdong Welding Institute (China-Ukraine E. O. Paton Institute of Welding), 510650 Guangzhou, China

<sup>2</sup>School of Materials Science and Engineering, Central South University, 410083 Changsha, China

**Abstract.** Transient liquid phase (TLP) bonding of Ni<sub>3</sub>Al-based superalloy IC10 was carried out using the interlayer based on the base metal which added B and Hf as the melting point depressant elements. The effect of bonding temperature (1250 – 1270 °C) on the microstructure evolution of bonding joints were investigated. Microstructure of bonding joint composed of isothermally solidification zone (ISZ) formed  $\gamma'$  phase and athermally solidified zone (ASZ) which consists of newly formed  $\gamma+\gamma'$  reticular eutectic among with borides and carbides. Boride precipitates are not formed in diffusion affected zone (DAZ) and the boundary between ASZ and ISZ become not obvious. Isothermally solidification rate decreases as the increase of the bonding temperature.

## 1 Introduction

Nickel-based superalloy is an essential material for the key parts of aero-engine working blades, turbine disks and combustion chambers. With the advance of aero-engine technology, inlet temperature of the turbine is continuously increasing, which makes service temperature and service life of the turbine blades face a stern challenge[1]. As the newly developed Ni<sub>3</sub>Al based superalloys, IC10 can be used as the material for advanced aero-engine fan with a service temperature up to 1100 °C[2]. Transient liquid phase (TLP) bonding is currently an optimized technology utilized for joining Ni-based superalloy, which combines the beneficial features of liquid phase joining and diffusion bonding techniques.

The directionally solidified superalloy IC10 contains 1.5 Wt.% Hf, which makes the alloy has excellent casting properties. In the late stage of solidification, Hf rich liquid show superior flow characteristics and good wettability. Hf also can strengthen the  $\gamma'$ (Ni<sub>3</sub>Al) phase and improve its corrosion resistance. Basing on the Ni-Hf phase diagram, an appropriate content of Hf can reduce the liquidus temperatures of the alloy, and interlayers using Hf as the only melting point depressant element also had been successfully applied to TLP bonding of nickel-base superalloys[3]. However, due to the larger atomic radius of Hf, it takes a long time to reduce its concentration in the joint region. In this study, in order to decrease content of B in interlayer, B and Hf were both used as MPD elements in TLP bonding of the directionally solidified superalloy IC10. Appropriate bonding temperature have an important influence on the

degree of isothermal solidification and the formation of phases and their morphology.

## 2 Experiment procedure

The directionally solidified superalloy IC10 is mainly composed of mesh  $\gamma$  and  $\gamma'$  phase. Besides, some sunflower shaped  $\gamma+\gamma'$  eutectic together with some TaC and HfC carbides distribute among mesh  $\gamma$  and  $\gamma'$  phase[4]. The chemical compositions of the base metal and the interlayer numbered BH2 are shown in Table 1. The interlayer was melting with WK-I non-consumable vacuum arc melting furnace. Its melting temperature range was tested by Germany-resistant STA409PC synchronous thermal analyzer. The solidus and liquidus temperature of the interlayer are 1172.1 °C and 1240.7 °C, respectively.

The TLP bonding operation was carried out in a United States CVI high vacuum diffusion furnace. According to DSC results of the interlayer alloy, the specimens were bonded at temperature of 1250, 1260, 1270 °C for holding time of 2 h. Then the 4, 6 and 8 h were respectively kept at 1250 °C. Samples were etched in a solution of HNO<sub>3</sub>+HF+Glycerin (1:2:1). Microstructural examinations were carried out using Nova NanoSEM 430 ultra-high resolution field emissions scanning electron microscope equipped with a beryllium window energy dispersive spectrometer (EDS) system. X-ray diffraction (XRD) analysis of phases present in the joint area was carried out using a PANalytical X'Pert Power X diffractometer equipped with a Cu-K $\alpha$  target. The wave length of Cu-K $\alpha$  radiation was 0.15406 nm.

**Table 1** IC10 and BH2 interlayer alloy chemical composition (wt.%)

Alloy	B	Hf	C	Al	Cr	Co	Mo	Ta	W	Ni
IC10	0.04-0.042	1.4-1.5	0.087-0.09	5.4-5.5	7.1-7.3	12.1-12.3	1.5-1.6	6.7-6.9	4.9-5.2	Bal.
BH2	2.4	2.6	0.087-0.09	5.4-5.5	7.1-7.3	12.1-12.3	1.5-1.6	6.7-6.9	4.9-5.2	Bal.

### 3 Result and discussion

#### 3.1 Effect of temperature on microstructure evolution of TLP bonded joint

According to previous experiments, B and Hf were used as the MPD elements of TLP bonding IC10, the bonding joint mainly consisted of three zones: isothermally solidification zone (ISZ), athermally solidified zone (ASZ) and base metal (BM). Fig. 1 shows SEM images of the joint TLP bonded at 1250, 1260 and 1270 °C for 2 h with BH2 interlayer. Fig. 2 shows the analysis of X-ray diffraction patterns from tensile strength fracture surfaces of the joint, it revealed that the joint is composed of Ni<sub>3</sub>Al, HfC, TaC, WB and Cr<sub>1.8</sub>W<sub>3.2</sub>B<sub>3</sub>. Due to the complex composition of borides, it mostly called borides in this paper. It can be seen from Fig. 1 (a) and (b), the joint bonded at 1250 °C mainly consists of cellular  $\gamma'$

phase. Besides, newly formed  $\gamma+\gamma'$  reticular eutectic and a small amount of W rich borides distribute in the cellular  $\gamma'$  phase. As can be seen from Fig. 1 (c) and (d), the cellular  $\gamma'$  phase is larger at 1260 °C, which is related to the presence of a large amount of Al in liquid phase and un-restricted growth of  $\gamma'$  phase. As growth rate of cellular  $\gamma'$  phase increased, the boundary between ASZ and ISZ become not obvious. With the progress of isothermal solidification, solute elements whose partition coefficient less than one ( $k<1$ ) discharged to the liquid front phase, resulting in the solute redistribution in the frontier enrichment of the solid-liquid interface. Although the latent heat of crystallization is released during the solidification of the Ni-based solid solution, the frontal solid-liquid interface is under a positive temperature gradient, and  $\gamma'$  phase interface is in a cell-like shape. Therefore, there is a definite component undercooling at the front of the interface. It can be seen from Fig. 1 (e) and (f) that the cellular  $\gamma'$  phase disappears at 1270 °C.

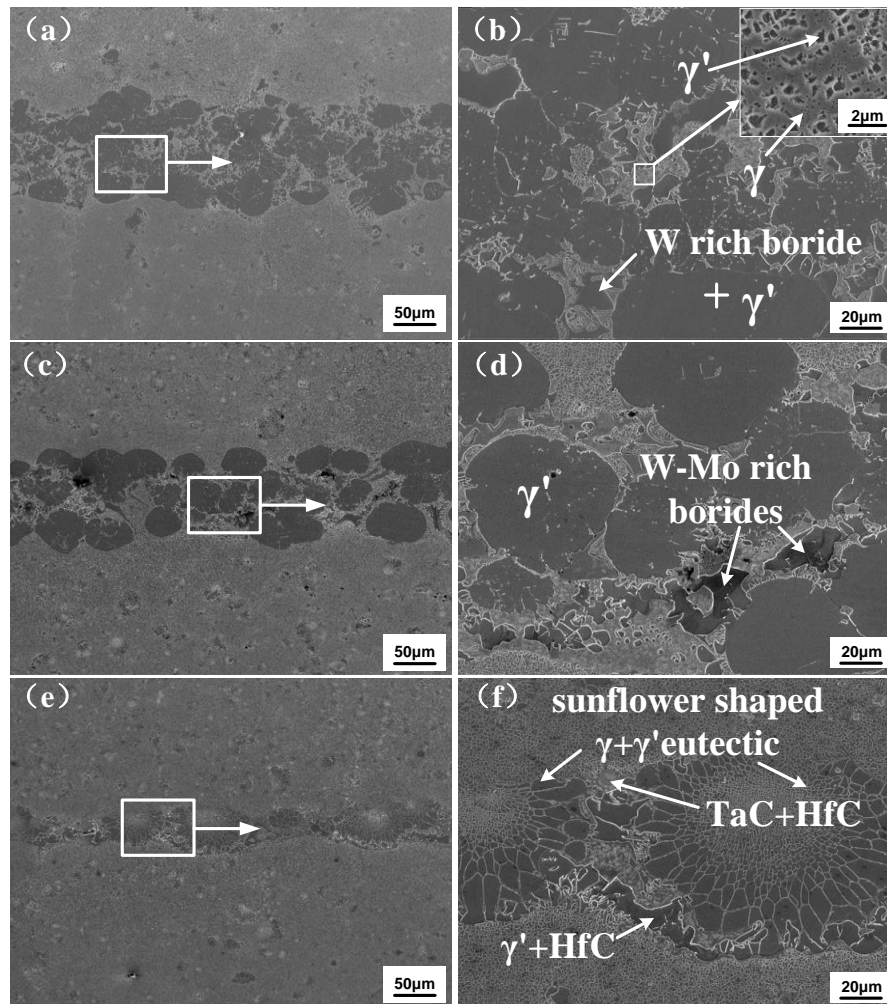


**Fig. 1.** SEM images of the joint TLP bonded at (a), (b) 1250 °C for 2 h; (c), (d) 1260 °C for 2 h; (e), (f) 1270 °C for 2 h.

The bonding joint mainly consists of sunflower shaped  $\gamma+\gamma'$  eutectic. Besides,  $\gamma'$  and HfC symbiotic phases, HfC and TaC symbiotic phases distribute at the edge of sunflower shaped eutectic.

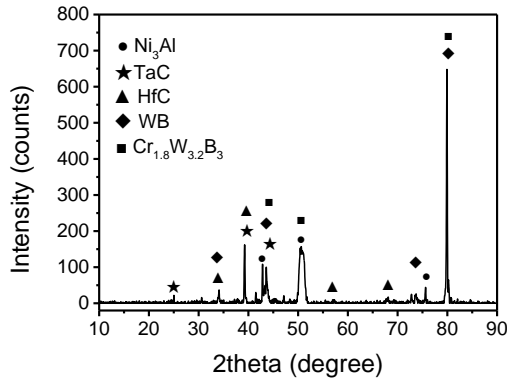


**Fig. 2.** XRD pattern of the tensile strength fracture surfaces of the TLP joint brazed at 1250 °C for 2 h.

It can be observed in Fig. 1, Boride precipitates are not formed in diffusion affected zone (DAZ) like conventional TLP bonding. This phenomenon also had been confirmed by M. Pouranvari[5] and A. Schnell[6]. Isothermal solidification process is controlled by diffusion of B to base metal. And the diffusion of B from the ISZ to base metal is controlled by the concentration of B in the liquid and ISZ interfaces. If B content in ISZ is lower than B solubility in the base metal, boride precipitation in the base metal would not be formed. In addition, Cr, W and Mo from the interlayer and the base metal are easily combined with B which leads to the decrease of B content in ISZ. Therefore, it is more difficult to form boride precipitates.

### 3.2 Effect of temperature on isothermal solidification rate of TLP bonded joint

It can be seen from Fig. 1, the isothermal solidification rate decreases as the increase of the bonding temperature. Cellular  $\gamma'$  phase become obvious as the bonding temperature rises from 1250 to 1260 °C. When the bonding temperature increases to 1270 °C, the degree of solidification is low and the sunflower shaped  $\gamma+\gamma'$  eutectic is formed. Jalilvand V et al.[7] believed that the low isothermal solidification rate is not only related to the enrichment of base metal alloy elements in the liquid phase, but also to the decrease of the solid solubility limit of B in base metal. Fick's second law ignores changes in D and concentration, and assumes a constant diffusion coefficient:

$$\frac{\partial c}{\partial t} = D \frac{\partial^2 c}{\partial x^2} \quad (1)$$

$\partial c / \partial t$  is the solid-liquid surface solid-state diffusion rate,  $D$  is the diffusion coefficient.  $\partial^2 c / \partial x^2$  is concentration gradient of MPD elements as the diffusion distance changes and is determined by the solid solubility limit of MPD elements in the base metal. The concentration gradient of MPD elements in the base metal affects diffusion rate, controlling the isothermal solidification rate. According to the Arrhenius equation,

an increase in temperature leads to an exponential increase in diffusion coefficient of MPD elements. Based on the Ni-B phase diagram, above the eutectic temperature, the solubility of B in Ni decreases with the increase of the bonding temperature. The decrease of the solubility of B in Ni leads to a decrease of the driving force for the diffusion of B at the solid-liquid interface, resulting in the enrichment of B in the liquid phase.

The rate of isothermal solidification also can be judged by the time required for isothermal solidification, which is controlled by the solid-phase diffusion of solute atoms. The diffusion problem can be treated as a diffusion matter in an infinite system with the width of  $2h = W_0$  ( $W_0$  is the thickness of the interlayer). The concentration of the diffusion element in the thickness of the interlayer is  $C_0$ , and the concentration of the other regions (the concentration of the diffusion element in the base metal) is  $C_m$ . From this, we can find the concentration distribution of diffusing elements in the system at a bonding temperature for a period of time. According to Fick's second law, we use the error function to solve[8, 9]:

$$C(x, t) = C_m + \frac{C_0 - C_m}{2} \left\{ \operatorname{erf} \frac{x+h}{2\sqrt{Dt}} - \operatorname{erf} \frac{x-h}{2\sqrt{Dt}} \right\} \quad (2)$$

Where  $C(x, t)$  is a function of distance  $x$  from the weld center and time  $t$ , and  $D$  is the diffusion coefficient of the diffusion element in the solid phase at base metal. From Eq. 2, the time  $t_f$  required for isothermal solidification can be obtained as the time when the diffusion element concentration in the interlayer decreases to the solidus concentration  $C_s$  at  $x = 0$ [10]:

$$C_s - C_m = C_0 - C_m \left\{ \operatorname{erf} \frac{h}{2\sqrt{Dt_f}} \right\} \quad (3)$$

the diffusion coefficient of MPD element in base metal ( $D$ ) depends on bonding temperature through the Arrhenius relationship:

$$D = D_0 \left( \frac{-Q}{RT} \right) \quad (4)$$

where  $R$  is the gas constant,  $Q$  is the apparent activation energy for diffusion of MPD element,  $D_0$  is the frequency factor. If Hf as MPD element, the time of complete isothermal solidification ( $t_f$ ) can be estimated from Eq. 2 and Eq. 4. Bergner indicated that the  $Q$  and  $D_0$  of Hf is 287 KJ/mol and  $1.8 \times 10^{-4} \text{ m}^2/\text{s}$  at the temperature range of 750 - 1150 °C; Kurtz reported that the  $Q$  and  $D_0$  of Hf is 272.1 KJ/mol and  $2 \times 10^{-4} \text{ m}^2/\text{s}$  at the temperature range of 750 - 1150 °C[11]. The diffusion activation energy of Hf is 272.1 - 287 KJ/mol. In this experiment, we take  $Q = 272.1 \text{ KJ/mol}$ ,  $D_0 = 2 \times 10^{-4} \text{ m}^2/\text{s}$ . When  $W_0 = 100 \text{ }\mu\text{m}$ ,  $C_0 = 2.6 \text{ wt.}\%$ ,  $C_m = 1.4 \text{ wt.}\%$ , the time required for isothermal solidification ( $t_f$ ) at 1250, 1260 and 1270 °C is 2.96, 3.55 and 4.72 h, respectively. If B as MPD element, the time of complete isothermal solidification ( $t_f$ ) can be estimated from Eq. 3 and Eq. 4. The diffusion activation energy of B is 248 kJ/mol and  $D_0$  is  $0.81 \text{ m}^2/\text{s}$ . When  $W_0 = 100 \text{ }\mu\text{m}$ ,  $C_0 = 2.4 \text{ wt.}\%$ ,  $C_m = 0$ , the time required for isothermal solidification at 1250, 1260 and 1270 °C is 1.99, 1.97 and 1.92 h, respectively. In view of the time required for the isothermal solidification of B diffusion from calculation, the increase of temperature has little effect on the time

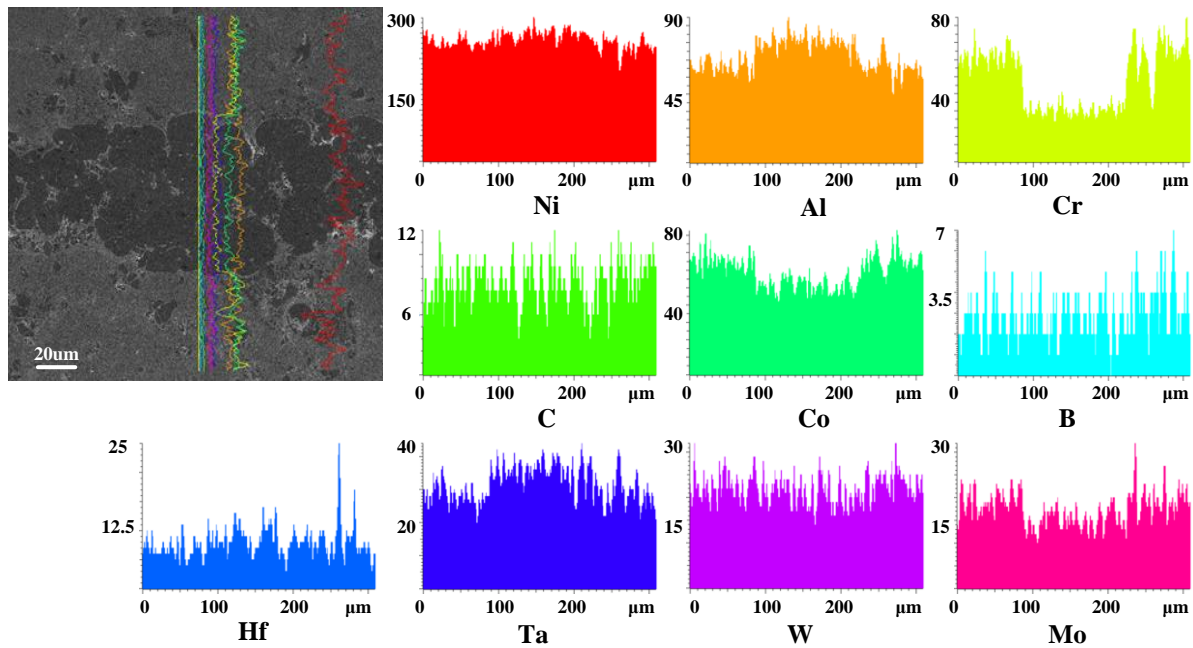


**Fig. 3.** SEM images in the TLP bonded sample brazed at 1250 °C for 4 h and it lines scan of Ni, Al, Cr, C, Co, B, Hf, Ta, W and Mo by SEM/EDS analysis.

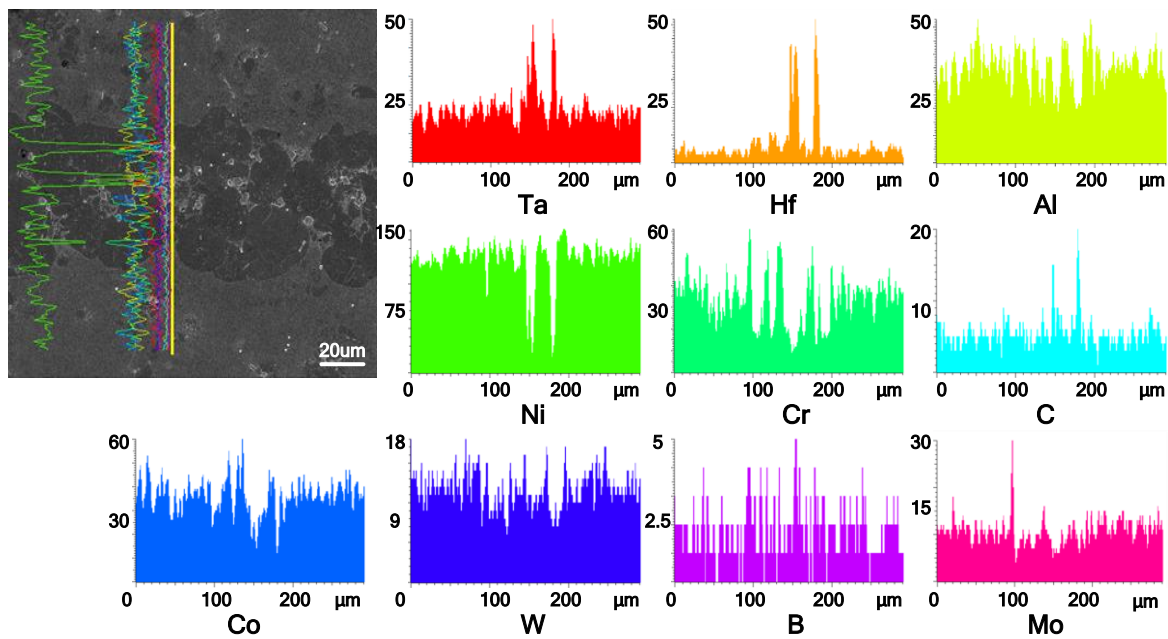


**Fig. 4.** SEM images in the TLP bonded sample brazed at 1250 °C for 8 h and it line scan of Ni, Al, Cr, C, Co, B, Hf, Ta, W and Mo by SEM/EDS analysis.

required to complete the isothermal solidification. However, the time required for the isothermal solidification of Hf diffusion depends strongly on bonding temperature. The time of complete isothermal solidification increased obviously, which indicates the decrease of isothermal solidification rate.

As can be seen from Fig. 3, the bonding joint almost completed the isothermal solidification at 1250 °C for 4 h. The distribution of Ni in bonded joint is uniform and content of Cr, Co, B, Mo and W is lower than that in base metal. It may be caused by Cr-W-Mo borides in the bonding region depleting Cr, Mo, W and B. However, Al, Ta and Hf in the bonding joint are higher than the base

metal because Hf and Ta elements tend to form carbides and preferentially enter  $\gamma'$  phase, and Al is the constituent of  $Ni_3Al$ . Fig. 4 shows the lines scan of the sample bonded at 1250 °C for 8 h. The peaks of Hf, Ta and C are in accord with each other, while the peaks of Ni and Al are exactly the opposite. It can be judged that the lines scan passes through the carbides riched Hf and Ta. Increasing the bonding time to 8 h, carbides and borides don't decrease in the bonding joint. This phenomenon can be explained by the higher Hf content in the interlayer, which forms carbides and is not easily decomposed at the bonding temperature. This is in agreement with the previous works on TLP bonding of

SXG3 alloy using Hf-containing Ni-based interlayer by Z.R. Yu et al.[3] who reported that granular Hf rich carbide was observed in the joint when the bonding time is 15 min. But the SXG3 alloy which bonded at 1290 °C for 6 h has been reheated to 1290 °C and quenched, Hf rich carbide still can be observed. According to quench results, carbides precipitated in the liquid phase at the bonding temperature, whereas the eutectic is formed in the bonding joint during the furnace cooling.

## 4 Conclusions

- (1) Microstructure of the TLP joint is composed of ISZ and ASZ. The ISZ formed  $\gamma'$  phase rather than the  $\gamma$  solid solution. The ASZ mainly consists of newly formed  $\gamma+\gamma'$  reticular eutectic, borides and carbides. Boride precipitates are not formed in DAZ like conventional TLP bonding.
- (2) The isothermal solidification rate decreases as the increase of the bonding temperature. Cellular  $\gamma'$  phase become obvious as the bonding temperature rises from 1250 to 1260 °C. When the bonding temperature increases to 1270 °C, the sunflower shaped  $\gamma+\gamma'$  eutectic structure is formed. When the bonding temperature is 1250 °C, prolonging holding time does not eliminate borides and carbides in the joint.

## Acknowledgments

This work was supported by the National International Science and Technology Cooperation Project of China (Grant No. 2015DFR50310), the Province Science and Technology Project of Guangdong (2017A070701026) and the 2018 GDAS' Special Project of Science and Technology Development (2018GDASCX-0113).

## References

1. S. Steuer, R.F. Singer, Metall, Mater. Trans. A. **45**, 3545 (2014)
2. H. Zhang, W. Wen, H. Cui, Mater. Sci. Eng. A. **504**, 99 (2009)
3. Z.R. Yu, X.F. Ding, N.M. Cao, Y.R. Zheng, F. Q. Acta Metall Sin. **52**, 549 (2016).
4. H. Zhang, W. Wen, H. Cui, Y. Xu, Mater. Sci. Eng. A. **527**, 328 (2009)
5. M. Pouranvari, A. Ekrami, A. Kokabi, Mater. Sci. Eng. A. **568**, 76 (2013)
6. M. Pouranvari, A. Ekrami, A.H. Kokabi, J. Alloy Compd. **469**, 270 (2009)
7. W. Gale, E. Wallach, Mater. Trans. A. **22**, 2451 (1991)
8. V. Jalilvand, H. Omidvar, M.R. Rahimipour, H.R. Shakeri, Mater Des. **52**, 36 (2013)
9. O.A. Idowu, N.L. Richards, M.C. Chaturvedi, Mater. Sci. Eng. A. **397**, 98 (2005)
10. M.A. Arafin, M. Medraj, D.P. Turner, P. Bocher, Adv. Mater. Res. **15**, 882 (2007)
11. O.A. Ojo, N.L. Richards, M.C. Chaturvedi, Sci.Technol. Weld. Join. **9**, 532 (2004)